

Direct current force sensing device based on compressive spring, permanent magnet, and coil-wound magnetostrictive/piezoelectric laminate

Cite as: Rev. Sci. Instrum. **84**, 125003 (2013); <https://doi.org/10.1063/1.4838615>

Submitted: 07 June 2013 . Accepted: 16 November 2013 . Published Online: 09 December 2013

Chung Ming Leung, Siu Wing Or, and S. L. Ho



View Online



Export Citation



CrossMark

ARTICLES YOU MAY BE INTERESTED IN

[High magnetoelectric effect at low magnetic basing in heterostructure rod of magnetostrictive fibers, piezoelectric tube, and epoxy binder](#)

Journal of Applied Physics **117**, 17D721 (2015); <https://doi.org/10.1063/1.4918574>

[Voltage-mode direct-current magnetoelectric sensor based on piezoelectric-magnetostrictive heterostructure](#)

Journal of Applied Physics **117**, 17A748 (2015); <https://doi.org/10.1063/1.4919047>

[Multiferroic magnetoelectric composites: Historical perspective, status, and future directions](#)

Journal of Applied Physics **103**, 031101 (2008); <https://doi.org/10.1063/1.2836410>



JANIS

Rising LHe costs? Janis has a solution.
Janis' Recirculating Cryocooler eliminates the use of Liquid Helium for "wet" cryogenic systems.

sales@janis.com www.janis.com [Click for more information.](#)



Direct current force sensing device based on compressive spring, permanent magnet, and coil-wound magnetostrictive/piezoelectric laminate

Chung Ming Leung, Siu Wing Or,^{a)} and S. L. Ho
 Department of Electrical Engineering, The Hong Kong Polytechnic University,
 Hung Hom, Kowloon, Hong Kong

(Received 7 June 2013; accepted 16 November 2013; published online 9 December 2013)

A force sensing device capable of sensing dc (or static) compressive forces is developed based on a NAS106N stainless steel compressive spring, a sintered NdFeB permanent magnet, and a coil-wound $\text{Tb}_{0.3}\text{Dy}_{0.7}\text{Fe}_{1.92}/\text{Pb}(\text{Zr}, \text{Ti})\text{O}_3$ magnetostrictive/piezoelectric laminate. The dc compressive force sensing in the device is evaluated theoretically and experimentally and is found to originate from a unique force-induced, position-dependent, current-driven dc magnetoelectric effect. The sensitivity of the device can be increased by increasing the spring constant of the compressive spring, the size of the permanent magnet, and/or the driving current for the coil-wound laminate. Devices of low-force (20 N) and high-force (200 N) types, showing high output voltages of 262 and 128 mV peak, respectively, are demonstrated at a low driving current of 100 mA peak by using different combinations of compressive spring and permanent magnet. © 2013 AIP Publishing LLC. [<http://dx.doi.org/10.1063/1.4838615>]

I. INTRODUCTION

The magnetoelectric (ME) effect in materials, especially the ME effect extrinsic in magnetostrictive/piezoelectric heterostructures, has been a hot research topic with numerous publications in the past decade.^{1–8} As a result, various interesting ME devices, including magnetic field sensors, current sensors, current-to-voltage converters, voltage-to-current converters, ME energy harvesters, magnetically tunable resonators, etc., have been fabricated and evaluated for new generation applications.^{9–16} From a physical perspective, the ME effect observed in the materials and utilized in the devices is essentially referred to the “ac” ME effect in which an applied ac magnetic field induces an ac voltage response through the coupled magneto-mechano-electric dynamics of the constituent magnetostrictive and piezoelectric phases of the materials.^{1–16} It is a pity that the materials and devices of this class suffer inherently from dc (or static) and even from quasi-dc (or quasi-static) operations.

In view of the deficiency and needs, a research interest has been shifted from the ac ME effect to the “dc” ME effect in recent years, and several studies have been reported on the dc ME effect extrinsic in magnetostrictive/piezoelectric, conductive/piezoelectric, and magnetic/conductive/piezoelectric heterostructures for dc magnetic field sensing.^{17–19} In those studies, an ac current or magnetic field of controlled amplitude and frequency has been introduced into the heterostructures as a driving signal for the induction of an ac voltage response upon an applied dc magnetic field. An interestingly high dc magnetic field sensitivity ranging from 0.3 to 17 $\mu\text{V}/\text{Oe}$ has been obtained at an ac driving current of 100 mA peak amplitude and 1 kHz frequency. The successful acquisition of the high sensitivity values has opened up an opportunity for competing with traditional Hall effect sensors

of 5–40 $\mu\text{V}/\text{Oe}$.²⁰ Nonetheless, device applications of the dc ME effect remain significantly less than those of the ac ME effect.

In this paper, we propose a promising type of dc (or static) compressive force sensing device formed by a nonmagnetic compressive spring, a permanent magnet, and a coil-wound magnetostrictive/piezoelectric laminate. The device features a unique force-induced, position-dependent, current-driven dc ME effect as a result of the dc compressive force-induced linear displacement (or contraction) governed by Hook’s law in the compressive spring, the position-dependent dc magnetic field generated by the permanent magnet, and the ac current-driven dc ME effect in the coil-wound laminate. The structure and working principle of the device are described and the force-induced, position-dependent, current-driven dc ME effect is evaluated theoretically and experimentally. The influence of spring constant, magnet size, and driving current on the sensitivity of the device is also discussed.

II. STRUCTURE AND WORKING PRINCIPLE

Figure 1 illustrates the schematic diagram and exploded view of the proposed dc compressive force sensing device. The device consists of a permanent magnet placed transversely on one end of a nonmagnetic compressive spring as well as a coil-wound magnetostrictive/piezoelectric laminate aligned and situated longitudinally inside the compressive spring at the other end, all supported by a pedestal. To enable the study of the influence of the compressive spring and permanent magnet on the sensitivity of the device, two different compressive springs and two different permanent magnets were used in the present work. The two compressive springs, namely, Springs I and II, were made by NAS106N stainless steel round wires of different diameters of 1.2 and 1.6 mm, respectively, and with their ends closed and ground. Spring

^{a)} Author to whom correspondence should be addressed. Electronic mail: eeswor@polyu.edu.hk

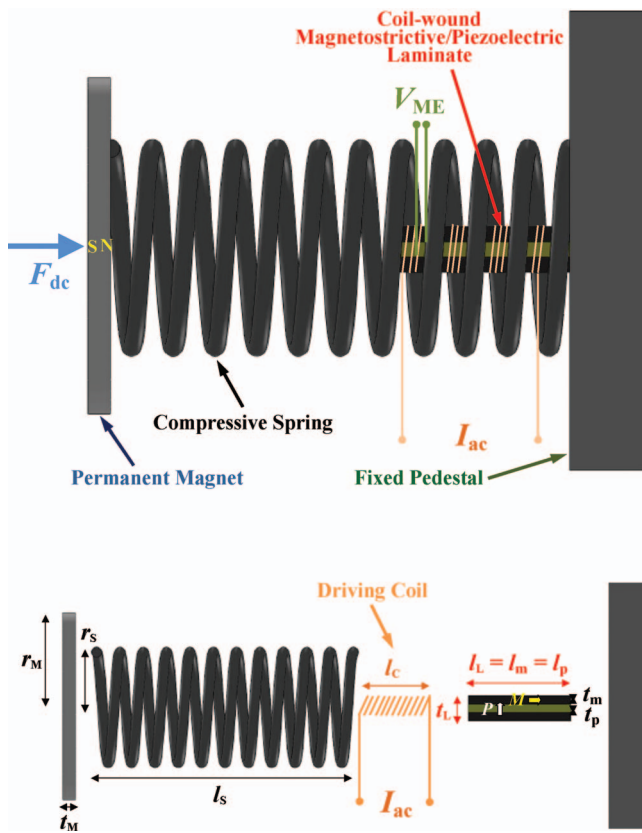


FIG. 1. Schematic diagram and exploded view of the proposed dc compressive force sensing device.

I had a mean radius (r_S) of 5.5 mm, a free length (l_S) of 30 mm, an active turn number (n_S) of 13, a pitch (p_S) of 2.4 mm, and a spring constant (k_S) of 1395 N/m, while Spring II had a larger r_S of 7.7 mm, a longer l_S of 38 mm, a smaller n_S of 7, a higher p_S of 7 mm, and a larger k_S of 11 091 N/m. The two permanent magnets, denoted as Magnets I and II, were made by sintered NdFeB in the form of a disk and with a nickel galvanization layer on the surface. Magnet I had a radius (r_M) of 7.5 mm and a thickness (t_M) of 1.5 mm, while Magnet II had an increased r_M of 11 mm and the same t_M of 1.5 mm. The north (N) and south (S) poles of both permanent magnets were normal to their circular main faces and their residual magnetic flux density (B_r) was known to be 1.12 T. The coil-wound magnetostrictive/piezoelectric laminate was a plate-shaped, longitudinally magnetized, transversely polarized magnetostrictive/piezoelectric laminated composite having a length (l_L) of 12 mm, a width (w_L) of 6 mm, a thickness (t_L) of 3 mm, and with a driving coil of 30 turns (n_C) and 12 mm length (l_C) wound on the composite using a brass round wire of 0.4 mm diameter. The upper and lower mag-

netostrictive layers were $\text{Tb}_{0.3}\text{Dy}_{0.7}\text{Fe}_{1.92}$ (Terfenol-D) alloy plates (Baotou Rare Earth Research Institute, China) with the highly magnetostrictive [112] crystallographic axis (M) oriented along their longitudinal direction. The central piezoelectric layer was P8 hard $\text{Pb}(\text{Zr}, \text{Ti})\text{O}_3$ (PZT) ceramic plate (CeramTec GmbH, Germany) with the electric polarization (P) direction along its thickness direction based on the two full fired silver electroded faces normal to the thickness. The Terfenol-D and PZT plates carried the same dimensions of 12 mm length ($l_m = l_p = l_L$), 6 mm width ($w_m = w_p = w_L$), and 1 mm thickness ($t_m = t_p$). Their useful material parameters are tabulated as shown in Table I.

The dc compressive force sensing device in Fig. 1 is operated on the basis of a force-induced, position-dependent, current-driven dc ME effect which, in other words, is a cooperative effect of the dc (or static) compressive force-induced linear displacement (or contraction) governed by Hook's law in the compressive spring, the position-dependent dc magnetic field generated by the permanent magnet, and the ac current-driven dc ME effect in the coil-wound magnetostrictive/piezoelectric laminate. In the absence of an applied dc compressive force ($F_{dc} = 0$ N), the permanent magnet, which is placed on one end of the compressive spring and separated from the transversal center of the coil-wound laminate with a zero-force effective distance ($l_S - l_L/2$), produces a zero-force effective distance (H_{dc0}) to the coil-wound laminate. The driving of an ac current (I_{ac}) of controlled amplitude and frequency into the driving coil of the coil-wound laminate induces an ac magnetic field (H_{ac}) along the longitudinal direction of the coil-wound laminate in accordance with Ampère's law. This H_{ac} , under the biasing of H_{dc0} , causes a zero-force ac ME voltage (V_{ME0}) at the output of the coil-wound laminate based on the coupled dynamics of the longitudinal magnetostrictive effect in the Terfenol-D plates and the transverse piezoelectric effect in the PZT plate. In the presence of F_{dc} , the linear displacement (u_{dc}) governed by Hook's law in the compressive spring shortens its free length (l_S) to ($l_S - u_{dc}$) and so its zero-force effective distance ($l_S - l_L/2$) to ($l_S - l_L/2 - u_{dc}$). This essentially moves the permanent magnet towards the coil-wound laminate, thereby increasing H_{dc0} to H_{dc} . In fact, an increase in H_{dc} means an increase in the magnetic biasing level for the coil-wound laminate. If H_{dc0} is small such that the subsequent increase in H_{dc} is within the linear positive magnetostrictive strain coefficient ($d_{33,m}$) region of the Terfenol-D plates in the coil-wound laminate,^{21–23} the driving of a controlled I_{ac} and hence a controlled H_{ac} into the coil-wound laminate will increase linearly V_{ME0} to V_{ME} though the I_{ac} -driven dc ME effect.

Theoretically, the dc compressive force (F_{dc})-induced linear displacement (u_{dc}) in the compressive spring can be

TABLE I. Measured material parameters of Terfenol-D and PZT plates used in the coil-wound magnetostrictive/piezoelectric laminate.

Terfenol-D	$d_{33,m} (\times 10^{-9}/\text{Oe})$	$s_{33}^H (\text{m}^2/\text{N})$		
	$28.7 \times 10^{-3} \cdot H_{dc}$	$(21.8 \times 10^9 - 6.58 \times 10^6 \cdot H_{dc})^{-1}$		
P8 PZT	$d_{31,p} (\text{pC}/\text{N})$	$\epsilon_{33}^T/\epsilon_0$	$s_{11}^E (\text{pm}^2/\text{N})$	k_{31}
	-95	1000	11.4	0.3

related to spring constant (k_S) and described by Hook's law as²⁴

$$u_{dc} = \frac{F_{dc}}{k_S}. \quad (1)$$

Based on the current model for analyzing solid cylindrical permanent magnets with uniform axial magnetization,²⁵ the position (u_{dc})-dependent dc magnetic field (H_{dc}) generated by the permanent magnet disk in the longitudinal direction and detected by the coil-wound laminate at an effective distance ($l_S - l_L/2 - u_{dc}$) can be expressed as

$$H_{dc} = \frac{B_r}{2} \left(\frac{l_S - l_L/2 - u_{dc} + t_M}{\sqrt{(l_S - l_L/2 - u_{dc} + t_M)^2 + r_M^2}} - \frac{l_S - l_L/2 - u_{dc}}{\sqrt{(l_S - l_L/2 - u_{dc})^2 + r_M^2}} \right). \quad (2)$$

Equation (2) indicates that the size (t_M and r_M) and material (B_r) of the permanent magnet also have great influence on H_{dc} . Using the constitutive piezomagnetic equations for the longitudinally magnetized Terfenol-D plates,²³ the constitutive piezoelectric equations for the transversely polarized PZT plate,²⁶ and Ampère's law for the current-carrying driving coil (i.e., $H_{ac} = n_C I_{ac} / l_C$),²⁷ the ac current (I_{ac})-driven dc ME effect in the coil-wound laminate can be derived as

$$V_{ME} = \frac{av(1-v)t_L d_{33,m} d_{31,p}}{\varepsilon_{33}^T [v s_{11}^E (1 - k_{31}^2) + (1-v) s_{33}^H]} \cdot \frac{n_C I_{ac}}{l_C}, \quad (3)$$

where a ($=0.5$) is a constant relating to the magneto-mechano-electric coupling in the coil-wound laminate;²⁸ $v = 2t_m/t_L$ is the volume fraction of the Terfenol-D plates in the coil-wound laminate; $d_{33,m}$ and s_{33}^H are the H_{dc} -dependent piezomagnetic strain coefficient and elastic compliance coefficient of the Terfenol-D plates, respectively; and $d_{31,p}$, k_{31} , s_{11}^E , and ε_{33}^T are the piezoelectric strain coefficient, electromechanical coupling coefficient, elastic compliance coefficient, and dielectric permittivity of the PZT plate, respectively. It is noted that F_{dc} induces u_{dc} in Eq. (1) based on Hooke's law in the compressive spring. This u_{dc} increases H_{dc} in Eq. (2) due to the u_{dc} -dependent nature of the permanent magnet. The increased H_{dc} , if within the linear positive $d_{33,m}$ region, increases linearly $d_{33,m}$ and s_{33}^H in the Terfenol-D plates (Table I) which, in turn, leads to a linear increase in V_{ME} under the driving of I_{ac} and hence H_{ac} in Eq. (3) because of the I_{ac} -driven dc ME effect in the coil-wound laminate. In short, we address this cooperative effect as the force-induced, position-dependent, current-driven dc ME effect which plays the governing role in the operation of our proposed dc compressive force sensing device.

III. RESULTS AND DISCUSSION

Figure 2 shows the measured dc magnetic field (H_{dc}) dependence of ac ME voltage (V_{ME}) of the coil-wound laminate detached from the dc compressive force sensing device in Fig. 1 and driven at an ac current (I_{ac}) of 100 mA

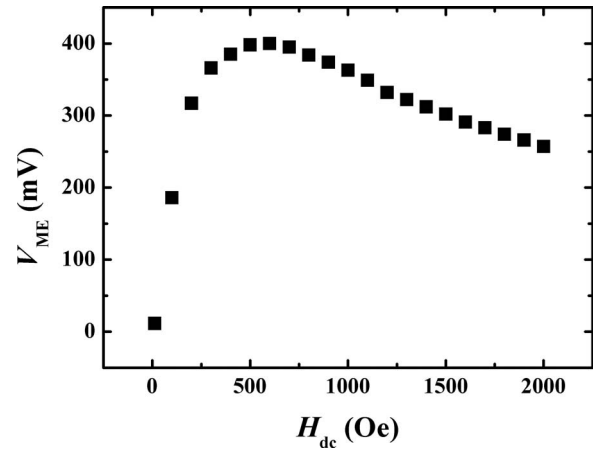


FIG. 2. Measured dc magnetic field (H_{dc}) dependence of ac ME voltage (V_{ME}) of the coil-wound laminate detached from the dc compressive force sensing device in Fig. 1 and driven at an ac current (I_{ac}) of 100 mA peak amplitude and 1 kHz frequency.

peak amplitude and 1 kHz frequency. H_{dc} of 20–2000 Oe was produced by a water-cooled, C-shaped electromagnet (Mylten PEM-8005k) under the energization of a dc current supply (Sorensen DHP200-15). I_{ac} was provided by an arbitrary waveform generator (Agilent 33210A) through a constant-current supply amplifier (AE Techron 7796HF). The resulting H_{ac} was monitored by a Hall effect probe connected to a Gaussmeter (F. W. Bell 7030). V_{ME} was measured by a digitizing oscilloscope (LeCory WaveRunner 44 Xi). It is clear that V_{ME} increases linearly in the initial range of H_{dc} of 0–300 Oe and reaches the maximum of 400 mV at 600 Oe before exhibiting a decreasing trend with increasing H_{dc} . It is known from Eq. (3) that V_{ME} is a function of both $d_{33,m}$ and s_{33}^H . It is also known from the magnetostrictive effect in magnetostrictive materials that $d_{33,m}$ and s_{33}^H are a function of H_{dc} (Table I).^{21–23} Therefore, the initial increase in V_{ME} with increasing H_{dc} is mainly caused by the H_{dc} -induced magnetostrictive strains in the linear positive $d_{33,m}$ region of the Terfenol-D plates in the coil-wound laminate. As H_{dc} is raised near 600 Oe, the elastic compliance associated with increased deformation is maximized, leading to the maximization in V_{ME} . Beyond this H_{dc} , constraining of magnetostrictive strains due to interaction with H_{dc} gives rise to a decrease in V_{ME} . Nonetheless, the initial linear response of V_{ME} to H_{dc} in the H_{dc} range of 0–300 Oe under a controlled I_{ac} (or H_{ac}) suggests a proper window of operation of our dc compressive force sensing device.

Figure 3 plots the measured (symbols) and calculated (lines) ac ME voltage (V_{ME}) as a function of dc compressive force (F_{dc}) of the dc compressive force sensing device under different combinations of ac current ($I_{ac} = 50$ and 100 mA peak at 1 kHz) [Fig. 3(a)], permanent magnet (Magnets I and II) [Fig. 3(b)], and compressive spring (Springs I and II) [Fig. 3(c)]. F_{dc} was provided by a C-shaped force clasper equipped with a load cell (HBM C9B) and an amplifier (Dacell AM-310), while I_{ac} and V_{ME} were supplied and measured by the same equipment used for Fig. 2. The calculated V_{ME} – F_{dc} curves, which were based on Eqs. (1)–(3), the material parameters shown in Table I, and the geometric parameters

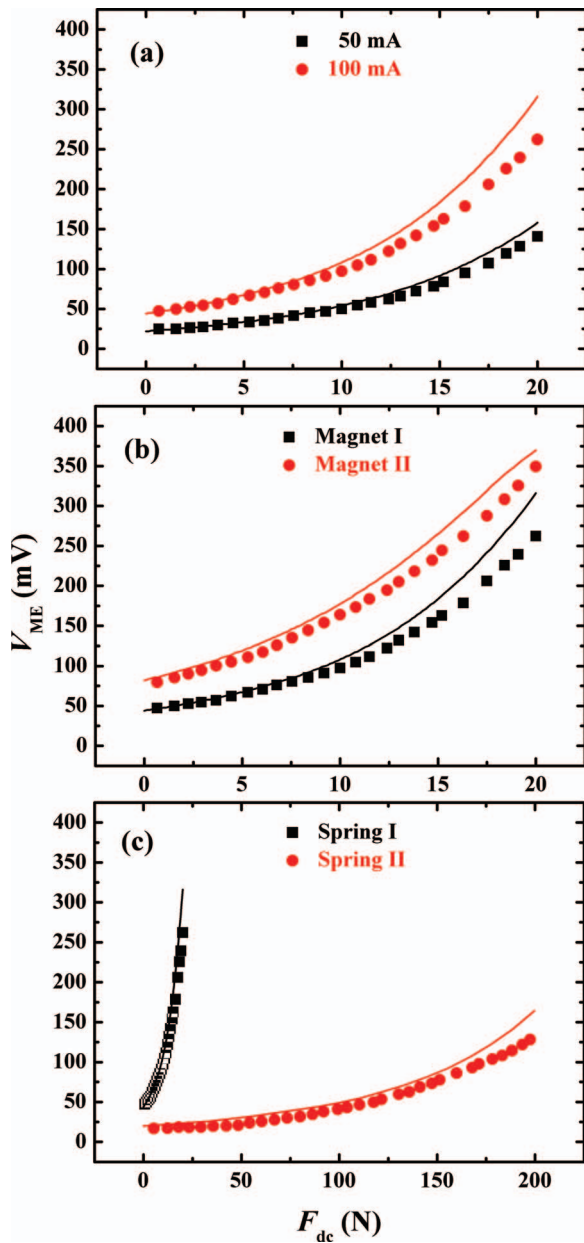


FIG. 3. Measured (symbols) and calculated (lines) ac ME voltage (V_{ME}) as a function of dc compressive force (F_{dc}) of the dc compressive force sensing device under different combinations of ac current (I_{ac} = 50 and 100 mA peak at 1 kHz), permanent magnet (Magnets I and II), and compressive spring (Springs I and II). (a) Effect of I_{ac} on $V_{ME}-F_{dc}$ curve when Magnet I and Spring I were used. (b) Effect of magnet size on $V_{ME}-F_{dc}$ curve when I_{ac} = 100 mA peak and Spring I were employed. (c) Effect of spring constant (k_s) on $V_{ME}-F_{dc}$ curve when I_{ac} = 100 mA peak and Magnet I were selected.

presented in Sec. II, are found to agree well with the measured $V_{ME}-F_{dc}$ curves for different combinations of I_{ac} , permanent magnets, and compressive springs. Figure 3(a) shows the effect of I_{ac} on the $V_{ME}-F_{dc}$ curve when the device was configured using Magnet I and Spring I. It is clear that V_{ME} increases with increasing F_{dc} in the 0–20 N range for a given I_{ac} . Increasing I_{ac} improves the whole V_{ME} response to F_{dc} in general. Figure 3(b) gives the influence of magnet size on the $V_{ME}-F_{dc}$ curve when I_{ac} = 100 mA peak and Spring I were employed. It is obvious that the use of a bigger per-

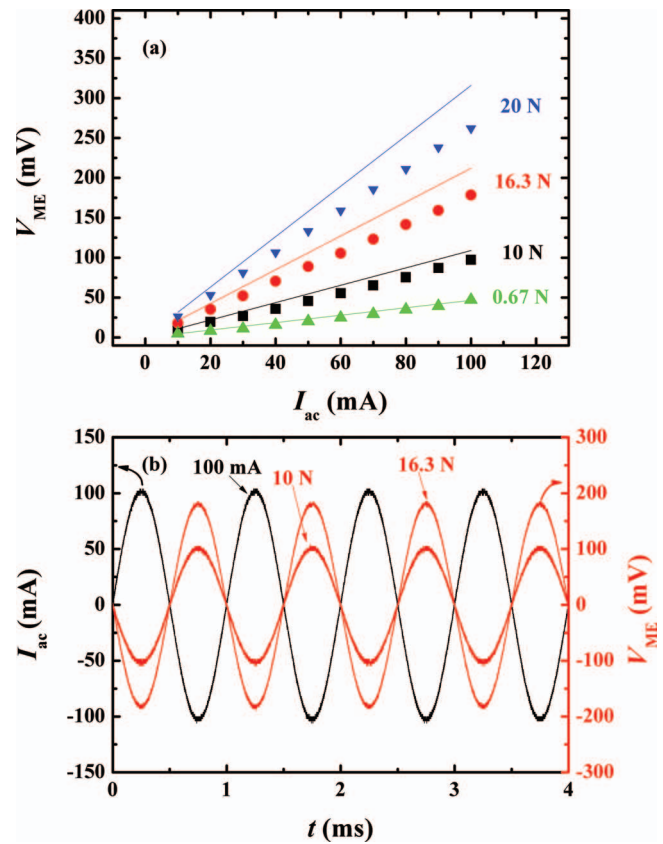


FIG. 4. (a) Measured and calculated ac ME voltage (V_{ME}) as a function of ac current (I_{ac}) of the dc compressive force sensing device configured with Magnet I and Spring I for various dc compressive forces (F_{dc}). (b) Waveforms of I_{ac} (=100 mA peak) and V_{ME} at two different F_{dc} of 10 and 16.3 N.

manent magnet (i.e., Magnet II) can effectively increase the V_{ME} response under the same F_{dc} in the F_{dc} range of 0–20 N. Figure 3(c) displays the effect of spring constant (k_s) on the $V_{ME}-F_{dc}$ curve when I_{ac} = 100 mA peak and Magnet I were selected. It is seen that k_s has a significant influence on the sensitivity of the $V_{ME}-F_{dc}$ curve. The use of a compressive spring of smaller k_s (=1395 N/m for Spring I) results in a low-force (20 N) device with a higher sensitivity (262 mV peak at 20 N), while the adoption of a compressive spring of larger k_s (=11091 N/m for Spring II) leads to a high-force (200 N) device with a lower sensitivity (128 mV peak at 200 N).

Figure 4(a) shows the measured (symbols) and calculated (lines) ac ME voltage (V_{ME}) as a function of ac current (I_{ac}) of the dc compressive force sensing device configured with Magnet I and Spring I for various dc compressive forces (F_{dc}). In agreement with Eq. (3), V_{ME} exhibits a linear relationship with I_{ac} for all levels of F_{dc} . Figure 4(b) illustrates the waveforms of I_{ac} (=100 mA peak) and V_{ME} at two different F_{dc} of 10 and 16.3 N. The stable signal conversion between I_{ac} and V_{ME} is apparent, further confirming the operation and performance of our proposed device. The 180° phase reversal between I_{ac} and V_{ME} is mainly caused by the negative sign carried by the piezoelectric coefficient $d_{31,p}$ in accordance with Eq. (3) and Table I.

IV. CONCLUSION

We have developed and evaluated a promising type of dc compressive force sensing device composed of a NAS106N stainless steel compressive spring, a sintered NdFeB permanent magnet, and a coil-wound Terfenol-D/PZT magnetostrictive/piezoelectric laminate. The theoretical and experimental results have confirmed the operation of the device in accordance with a unique force-induced, position-dependent, current-driven dc ME effect as well as the increase in sensitivity by increasing the spring constant of the compressive spring, the size of the permanent magnet, and/or the driving current for the coil-wound laminate. By suitably combining compressive spring and permanent magnet, a low-force (20 N) device and a high-force (200 N) device, possessing high output voltages of 262 and 128 mV peak, respectively, have been demonstrated at a low driving current of 100 mA peak. The present work not only proposes a new generation form of dc compressive force sensing device, but also extends device applications of the dc ME effect.

ACKNOWLEDGMENTS

This work was supported by the Research Grants Council of the HKSAR Government (PolyU 5228/13E) and The Hong Kong Polytechnic University (H-ZG76 and 1-ZV7P).

- ¹J. Ryu, S. Priya, A. V. Carazo, K. Uchino, and H. E. Kim, *J. Am. Ceram. Soc.* **84**, 2905 (2001).
- ²N. Nersessian, S. W. Or, and G. P. Carman, *IEEE Trans. Magn.* **40**, 2646 (2004).
- ³M. Fiebig, *J. Phys. D* **38**, R123 (2005).
- ⁴Y. M. Jia, S. W. Or, J. Wang, H. L. W. Chan, X. Y. Zhao, and H. S. Luo, *J. Appl. Phys.* **101**, 104103 (2007).
- ⁵H. F. Zhang, S. W. Or, and H. L. W. Chan, *J. Appl. Phys.* **104**, 104109 (2008).
- ⁶S. Peng, P. Yang, W. Cai, X. M. Lu, J. M. Liu, F. Yan, M. Xu, H. J. Zhang, J. Y. Wang, and J. S. Zhu, *J. Appl. Phys.* **105**, 061622 (2009).
- ⁷C. Y. Lo, S. H. Choy, S. W. Or, and H. L. W. Chan, *J. Appl. Phys.* **107**, 093907 (2010).
- ⁸Y. F. Duan, C. M. Leung, S. Y. Zhang, L. Zhang, and S. W. Or, *J. Appl. Phys.* **111**, 07C717 (2012).
- ⁹S. Priya, R. Islam, S. X. Dong, and D. Viehland, *J. Electroceram.* **19**, 149 (2007).
- ¹⁰C. W. Nan, M. I. Bichurin, S. X. Dong, D. Viehland, and G. Srinivasan, *J. Appl. Phys.* **103**, 031101 (2008).
- ¹¹Y. M. Jia, S. W. Or, H. L. W. Chan, J. Jiao, H. S. Luo, and S. van der Zwaag, *Appl. Phys. Lett.* **94**, 263504 (2009).
- ¹²Y. J. Wang, X. Y. Zhao, W. N. Di, H. S. Luo, and S. W. Or, *Appl. Phys. Lett.* **95**, 143503 (2009).
- ¹³C. M. Leung, S. W. Or, S. Y. Zhang, and S. L. Ho, *J. Appl. Phys.* **107**, 09D918 (2010).
- ¹⁴C. M. Leung, S. W. Or, F. F. Wang, S. L. Ho, and H. S. Luo, *Rev. Sci. Instrum.* **82**, 013903 (2011).
- ¹⁵Y. J. Wang, D. Gray, D. Berry, J. Q. Gao, M. H. Li, J. F. Li, and D. Viehland, *Adv. Mater.* **23**, 4111 (2011).
- ¹⁶S. Y. Zhang, C. M. Leung, W. Kuang, S. W. Or, and S. L. Ho, *J. Appl. Phys.* **113**, 17C733 (2013).
- ¹⁷Y. M. Jia, Y. X. Tang, X. Y. Zhao, H. S. Luo, S. W. Or, and H. L. W. Chan, *J. Appl. Phys.* **100**, 126102 (2006).
- ¹⁸C. M. Leung, S. W. Or, and S. L. Ho, *J. Appl. Phys.* **107**, 09E702 (2010).
- ¹⁹L. Zhang, C. M. Leung, S. W. Or, and S. L. Ho, *J. Appl. Phys.* **114**, 027016 (2013).
- ²⁰E. Ramsden, *Hall-Effect Sensors: Theory and Applications*, 2nd ed. (Elsevier, Burlington, Oxford, 2006).
- ²¹S. W. Or, N. Nersessian, G. P. McKnight, and G. P. Carman, *J. Appl. Phys.* **93**, 8510 (2003).
- ²²S. W. Or, N. Nersessian, and G. P. Carman, *IEEE Trans. Magn.* **40**, 71 (2004).
- ²³T. M. Atanackovic, *Theory of Elasticity for Scientists and Engineers* (Birkhäuser, Boston, 2000).
- ²⁴E. P. Furlani, *Permanent Magnet and Electromechanical Devices: Materials, Analysis, and Applications* (Academic, San Diego, 2001).
- ²⁵G. Engdahl, *Magnetostrictive Materials Handbook* (Academic, NY, 2000).
- ²⁶T. Ikeda, *Fundamentals of Piezoelectricity* (Oxford University Press, Oxford, 1990).
- ²⁷R. F. Harrington, *Introduction to Electromagnetic Engineering* (Mineola, NY, 2003).
- ²⁸S. X. Dong, J. F. Li, and D. Viehland, *IEEE Trans. Ultrason. Ferroelectr. Freq. Control* **50**, 1253 (2003).